








AKADÉMIAI KIADÓ

Differential transcriptome profile underlying risky choice in a rat gambling task

MYUNG JI KWAK^{1†} , WHA YOUNG KIM^{2†} ,
SEUNG-HYUN JUNG^{3,4,5*} , YEUN-JUN CHUNG^{4,5,6*}  and
JEONG-HOON KIM^{1,2*} 

Journal of Behavioral Addictions

11 (2022) 3, 845–857

DOI:

[10.1556/2006.2022.00068](https://doi.org/10.1556/2006.2022.00068)

© 2022 The Author(s)

¹ Department of Medical Sciences, Graduate School of Medical Science, Brain Korea 21 Project, Yonsei University College of Medicine, Seoul 03722, South Korea

² Department of Physiology, Yonsei University College of Medicine, Seoul 03722, South Korea

³ Department of Biochemistry, Cancer Evolution Research Center, The Catholic University of Korea College of Medicine, Seoul 06591, South Korea

⁴ Department of Biomedicine & Health Sciences, The Catholic University of Korea College of Medicine, Seoul 06591, South Korea

⁵ Precision Medicine Research Center, The Catholic University of Korea College of Medicine, Seoul 06591, South Korea

⁶ Department of Microbiology, IRCGP, The Catholic University of Korea College of Medicine, Seoul 06591, South Korea

FULL-LENGTH REPORT



Received: December 27, 2021 • Revised manuscript received: July 20, 2022 • Accepted: August 22, 2022

Published online: September 12, 2022

ABSTRACT

Background and aims: Proper measurement of expected risk is important for making rational decisions, and maladaptive decision making may underlie various psychiatric disorders. However, differentially expressed genetic profiling involved in this process is still largely unknown. A rodent version of the gambling task (rGT) has been developed to measure decision-making by adopting the same principle of Iowa Gambling Task in humans. In the present study, we examined using next-generation sequencing (NGS) technique whether there are differences in gene expression profiles in the medial prefrontal cortex (mPFC) and the nucleus accumbens (NAc) when rats make different choices toward risk in rGT. **Methods:** Rats were trained in a touch screen chamber to learn the relationships between 4 different light signals on the window of the screen and accompanied reward outcomes or punishments set up with different magnitudes and probabilities. Once they showed a stabilized pattern of preference upon free choice, rats were classified into risk-averse or risk-seeking groups. After performing the rGT, rats were decapitated, the mPFC and the NAc was dissected out, and NGS was performed with the total RNA extracted. **Results:** We found that 477 and 36 genes were differentially expressed (approximately 75 and 83% out of them were downregulated) in the mPFC and the NAc, respectively, in risk-seeking compared to risk-averse rats. Among those, we suggested a few top ranked genes that may contribute to promoting risky choices. **Discussion and conclusions:** Our findings provide insights into transcriptional components underlying risky choices in rats.

KEYWORDS

rat gambling task, risky choice, medial prefrontal cortex, transcriptome

[†]These authors contributed equally to this work.

*Corresponding authors.

E-mail: hyun@catholic.ac.kr, yejun@catholic.ac.kr, jkim1@yuhs.ac

INTRODUCTION

Efficient decision-making that maximizes long-term benefits in our lives is vital for the survival and well-being of individuals. In contrast, poor decision-making has detrimental effects on our lives, as demonstrated in individuals with gambling disorder and substance addiction. One of the characteristic core components of gambling disorders, similar to substance



addiction, is making continuous risky choices despite their adverse effects (Fauth-Buhler, Mann, & Potenza, 2017; Frascella, Potenza, Brown, & Childress, 2010; Potenza, 2008). To assess decision-making in humans, the Iowa gambling task (IGT) was developed as a simulated gambling task reflecting the complexity of the choices (Bechara, 2003; Bechara, Damasio, Damasio, & Anderson, 1994). It has been widely used to measure and analyze the choice behaviors in humans with various psychiatric conditions. By adopting the basic principles and structures of IGT, a similar rat version of the gambling task (rGT) has been developed in a few laboratories (de Visser, Homberg, et al., 2011; Kim, Cho, Kwak, & Kim, 2017; Rivalan, Ahmed, & Dellu-Hagedorn, 2009; Van den Bos, Koot, & de Visser, 2014; Zeeb, Robbins, & Winstanley, 2009). Some features of rGT commonly shared with IGT include uncertainty, reward, and punishment, making it a promising animal model for psychiatric disorders with decision-making deficits, including gambling disorder (Potenza, 2009; Van den Bos et al., 2014).

It has been reported that vulnerability to gambling disorder has a genetic basis, as shown by studies that include families and twins (Black, Monahan, Temkit, & Shaw, 2006; Ducci & Goldman, 2012; Lobo & Kennedy, 2009; Piasecki, Gizer, & Slutske, 2019; Slutske et al., 2000). Similarly, studies including twins have shown that risk-taking behavior is also inheritable (Anokhin, Golosheykin, Grant, & Heath, 2009). Furthermore, a few genome-wide association studies have implicated some genes in gambling disorders (Lind et al., 2012; Lang et al., 2020). With the advances in RNA sequencing technologies, whole-transcriptome analysis for psychiatric disorders, including drug addictions, has become popular (Huggett & Stallings, 2020; Navandar et al., 2021; Walker et al., 2018). Although a report examined the mRNA expression levels in the brain obtained from rGT rats by *in situ* hybridization (Lobo et al., 2015), a whole-transcriptome analysis for these brains has not yet been conducted. Based on these findings, we hypothesized that there might be differences in the transcription levels in the rat brain reflecting differentiated characteristics in rGT. To test this hypothesis, we performed whole-transcriptome sequencing (WTS) of brain samples from rGT rats, targeting two brain regions, the medial prefrontal cortex (mPFC) and the nucleus accumbens (NAc), which are known to play important roles in decision-making and addictive disorders (de Visser, Baars, van't Klooster, & van den Bos, 2011; Fellows & Farah, 2005; Goto & Grace, 2008; Kim, Jang, Lee, Jang, & Kim, 2013; Orsini et al., 2018).

METHODS

Subjects

Male Sprague-Dawley rats, 3 weeks old on arrival, were obtained from Orient Bio Inc. (Seongnam-si, Korea). The rats were housed three per cage for 1-week to allow habituation to a new colony environment, during which they were handled by experimenters, and had access to food

ad libitum. Subsequently, they were housed two per cage and placed on a restricted diet with 85% of their normal daily food consumption, which was started 2 days before the pre-training experiments and maintained until the end of experimentation. After the daily training session, food was provided immediately to sufficiently maintain the animals' growth and motivation. Water was available *ad libitum* at all times. Colony rooms had a controlled room temperature (21 °C) and a 12-h light/dark cycle (lights on at 8:00 am), and all experiments were conducted during the day.

Apparatus

The rGT was conducted in a set of eight identical touchscreen-based automated operant chambers housed in dense sound- and light-attenuating boxes (68.6 cm high × 60.7 cm long × 53.5 cm wide) (Campden Instruments Ltd., Leics, UK). Each chamber was equipped with a house light (light-emitting diode), touch-sensitive liquid crystal display monitor (touchscreen; 15.0 inch, screen resolution 1,024 × 768), pellet dispenser, and food magazine unit (with light and infrared beam to detect entries) facing the touchscreen. The chambers had a trapezoidal shape (30 cm high × 33 cm long [from screen to magazine] × 25 cm wide for the screen and 13 cm wide for the magazine) (Fig. 1), which was designed to help focus the animal's attention on the touchscreen and reward delivery area (i.e., the food magazine) (Mar et al., 2013). On top of the chamber, a transparent lid was secured to the trapezoidal walls with latches to retain the animals inside the chambers. The floor was constructed from perforated stainless steel, and a tray for collecting litter was located below the floor. The touchscreen used sensitive optical infrared sensors that allowed the screen to reliably detect an animal's touch without pressure. A black plastic mask (36 cm high × 28 cm wide) with five response windows (the size of each window was 3.0 cm high × 3.0 cm wide, positioned in a row with the windows spaced 1.0 cm apart, 3.5 cm from the grid floor) was fitted in front of the touchscreen, which helped reduce accidental screen touches and clearly distinguish the response locations from the background. The visual stimulus, a solid white square, was shown only through the two left and two right response windows, the middle window was left black. We used the Whisker Standard Software (Campden Instruments, Ltd., Leics, UK) (Cardinal & Aitken, 2010) as the controlling software, and the four chambers were controlled using two computers each.

rGT pre-training

Animals were trained once daily in a 30 min session, 5 days per week. Sucrose pellets (45 mg) (Bio-Serve, Flemington, NJ, USA) were used as a reward. In stage 1, the animals were first habituated to the touchscreen chamber for one session. In stages 2 and 3, which lasted over five daily sessions, animals were trained to learn the relationship between the light stimulus on the screen and the reward pellet, and to touch the screen to receive a pellet as a reward. In this stage, the inter-trial interval (ITI) of the 5 s rule was first applied such



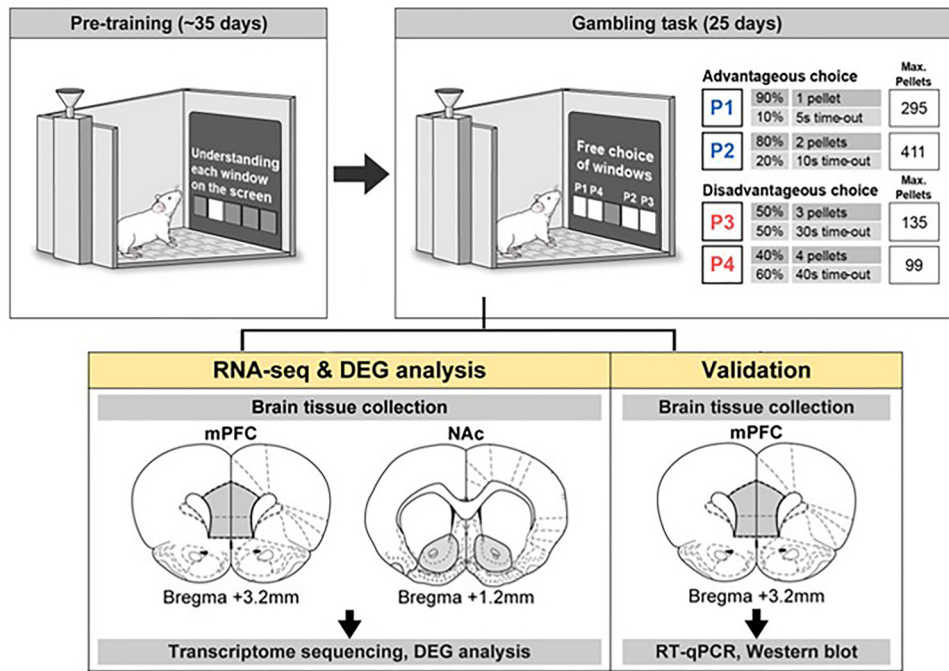


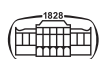
Fig. 1. Schematic illustration of the experimental procedures. (Top) Schematic diagram of the rGT chamber. P1~P4 indicate the windows on the screen. The number of pellets as rewards and time-outs as punishments together with their corresponding probabilities are shown on the right. In addition, the hypothetical calculation of the maximum number of pellets that rats would obtain during the 30-min trial is shown. (Bottom) A DEG analysis was conducted with the mPFC and the NAc regions, while validation experiments were performed only with the mPFC of the brains obtained from rGT rats

that animals had to wait for 5 s after pushing their noses into the food magazine to start a new trial. In stage 4, which lasted over 16 to 18 daily sessions, animals serially learned to touch one of the four windows which was randomly lit, within different stimulus durations (starting from 60 s, then serially reduced to 30, 20, and finally, 10 s), to receive one pellet. Animals completed the task either within 100 trials or 30 min, whichever came first. In this stage, they learned for the first time that they were punished with a time-out (i.e., the white house-light was lit for 5 s) if they touched the screen without waiting during ITI (premature) or if they did not touch the screen within the stimulus duration (omission). They were also punished if they touched other windows which were not lit. When the accuracy, which is defined as the number of correct touches divided by a total number of touches within different stimulus duration times, was greater than 80% and omissions were fewer than 20%, the animals were considered to have acquired the task.

rGT training

Essentially, during rGT training, the animals were confronted with four choices differing in their probability and magnitude of reward (food) and punishment (time-out), and they had to learn an optimal strategy to determine the choice that provided the most reward per session (Zeeb et al., 2009). In stage 5, which lasted over 7 daily sessions, the animals learned for the first time the relationship between each window and the reward/punishment ratio assigned to

that window, which was as follows: window (P1), 1 pellet (90%) or 5 s time-out (10%); window (P2), 2 pellets (80%) or 10 s time-out (20%); window (P3), 3 pellets (50%) or 30 s time-out (50%); and window (P4), 4 pellets (40%) or 40 s time-out (60%). In this stage, one of the four windows was randomly lit for 10-s and animals were punished (i.e., the white house light was lit for 5 s) for a premature response. Additionally, for the first time in this stage, animals were punished (time-out; i.e., the white house light was lit, and all the windows on the screen simultaneously flashed for 5–40 s) even on correctly touching the screen according to the pre-designated schedule for each window. So far, from stages 1–5, only one of the four windows on the screen was randomly lit. However, in stage 6, all four windows were simultaneously lit when each new trial started, and animals were allowed to wait for an ITI of 5 s of and then choose one of the four windows, which were lit for 10 s. The reward and punishment settings designated for each window were the same as those introduced in stage 5. Depending on which window the animals chose, they would receive either reward (pellet) or punishment (time-out) with differently programmed probabilities. Once a trial was finished, regardless of the outcome, they again encountered four different choices in the next trial, and this process was repeated for 30 min. Hypothetically, if one window was chosen exclusively, the amount of reward pellets per session that an animal could obtain was as follows: P1, 295; P2, 411; P3, 135; and P4, 99 pellets (Baarendse, Winstanley, & Vanderschuren, 2013). The percentage of choices ([number of



choices for a specific window divided by the total number of choices made] $\times 100$) was used to measure the animals' preferences for the different windows. After 25 daily sessions were completed, the average of the last three daily sessions' choice percentages was considered a basal score for the animals' risk-preference. Animals were categorized as risk-averse when their basal score for P1+P2 (advantageous choices) was equal to or higher than 60%, whereas they were categorized as risk-seeking when their basal score for P3+P4 (disadvantageous choices) was equal to or higher than 60%. When they were not classified into either risk-averse or risk-seeking, they were categorized as intermediate. To avoid any location bias, windows were allocated in a counterbalanced way as follows: for half of the animals, the windows were 1 (P1), 2 (P4), 3 (P2), and 4 (P3); for the other half of the animals, the windows were 1 (P4), 2 (P1), 3 (P3), and 4 (P2).

In addition to premature response and omission (both were expressed as a percentage of the total number of trials initiated), other choice-related behavioral parameters, such as choice latency (the time required for animals to correctly touch the screen, after the end of the ITI, while the screen was lit), reward collection latency (the time required for animals to obtain the reward after a correct screen touch), pause after loss timeout (the time elapsed for animals to enter food magazine after loss timeout), perseverative response (the number of either all or a single window touches per 5 s during timeout), feed-tray entry ITI (the number of feed-tray entries during ITI divided by total number of trials initiated) were analyzed.

Whole transcriptome sequencing

To identify transcriptional components that promote risky choice in rats, we performed WTS with total RNA extracted from the two brain regions (mPFC and NAc) of rGT trained rats. Total RNA was extracted using the miRNeasy Mini kit (Qiagen, Hilden, Germany), and its quantity and quality were measured using the Qubit (Thermo Fisher Scientific, Waltham, MA, USA) and TapeStation (Agilent Technologies, Santa Clara, CA, USA), respectively. Normally WTS is performed when the RNA Integrity Number (RIN) value is greater than or equal to 7. In the present study, we did not use RIN values as a covariate in differentially expressed gene (DEG) analysis because the quality of all extracted RNAs was high enough for WTS (average RIN value was 8.4 with a range of 8.1–8.8; see [Supplementary Table 1](#)). Extracted RNA was then converted into a cDNA library using TruSeq RNA Library Preparation Kit v2 (Illumina, San Diego, CA, USA). After polymerase chain reaction (PCR) amplification, the final product was assessed with a TapeStation (Agilent Technologies, Santa Clara, CA, USA) and subsequently sequenced on the Illumina NovaSeq 6000 platform (Illumina, San Diego, CA, USA) with 101-bp paired-end reads. Raw sequence data were first filtered and trimmed using Trimmomatic software ([Bolger, Lohse, & Usadel, 2014](#)). The sequencing reads were then mapped onto the *rattus norvegicus* reference genome (Rnor_6.0, rn6) using the STAR aligner v2.5.3a ([Dobin et al., 2013](#)). Gene-level quantification

of expression was performed with HTSeq v0.9.0 ([Anders, Pyl, & Huber, 2015](#)), according to the Ensembl transcript annotation (Rnor_6.0.91 version). Details of the WTS data are available in [Supplementary Table 1](#). DEG analyses were performed for gene sets with expression by the use of SARTools ([Varet, Brillet-Guéguen, Coppée, & Dillies, 2016](#)) and edgeR R package ([Robinson, McCarthy, & Smyth, 2010](#)). DEGs were defined by adjusted *P*-value by false discovery rate (*q*-value) of <0.1 and 1.3 times of fold change (i.e., $\log_2(1.3) = 0.38$ for up-regulated and $\log_2(\frac{1}{1.3}) = -0.38$ for down-regulated genes). The transcriptome sequencing data were deposited in the Gene Expression Omnibus database (GSE181296). Gene ontology (GO) enrichment analysis was performed using Metascape ([Zhou et al., 2019](#)). The 'biological process', 'cellular components', 'molecular function', and 'Kyoto Encyclopedia of Genes and Genomes (KEGG) pathways' categories were used in this analysis with default parameters (Min Overlap = 3, *P* Value Cutoff = 0.01, Min Enrichment = 1.5). Protein-protein interaction (PPI) network analysis was performed using Metascape and the molecular complex detection (MCODE) algorithm ([Bader & Hogue, 2003](#)) with default parameters (Databases: Physical Core, Min Network Size: 3, Max Network Size: 500).

Reverse transcription quantitative PCR

To validate DEGs conspicuously down-regulated in risk-seeking compared to risk-averse group of rats, we performed reverse transcription-quantitative PCR (RT-qPCR) with total RNA samples obtained in the half side of mPFC from an independent replication set of rGT trained rats. We designed multiple target-specific amplification primers for RT-qPCR and their detailed sequences are available in [Supplementary Table 2](#). Total RNA (500 ng) was reverse transcribed using oligo dT primers and SuperScript III reverse transcriptase (Thermo Fisher Scientific, Waltham, MA, USA). RT-qPCR was then performed with the ViiA 7 Real-Time PCR System (Thermo Fisher Scientific, Waltham, MA, USA) using THUNDERBIRD SYBR qPCR Mix (Toyobo, Osaka, Japan) and the target specific primer sets. Reaction mixture (10 μ L) was consisted of 1 μ L of cDNA, 5 μ L of THUNDERBIRD SYBR qPCR Mix, 1 μ L of 0.1X ROX dye, and 6 pmole of forward and reverse primer each. Thermal cycling conditions were as following: one cycle of 1 min at 95 °C followed by 40 cycles of 5 s at 95 °C, 10 s at 61 °C, and 20 s at 72 °C. Quantification of the relative expression was calculated using the $2^{-\Delta\Delta Ct}$, where ΔCt is the difference in threshold cycles for the sample in question normalized against the reference gene (*Gapdh*) and expressed relative to the value obtained by the calibrator (individual/calibrator) ([Jung et al., 2014](#)). All RT-qPCR experiments were triplicated.

Western blotting

To further validate DEGs conspicuously down-regulated in risk-seeking compared to risk-averse group of rats, we performed western blotting experiment with protein samples obtained in the half side of mPFC from the same



rGT trained rats used for RT-qPCR validation. Tissues were homogenized in lysis buffer (pH 7.4) containing 0.32 M sucrose, 2 mM EDTA, 1% SDS, 10 $\mu\text{g mL}^{-1}$ aprotinin, 10 $\mu\text{g mL}^{-1}$ leupeptin, 1 mM phenylmethylsulfonyl fluoride, 10 mM sodium fluoride, and 1 mM sodium orthovanadate. The concentration of protein was determined by using Pierce BCA Protein Assay Kit (Thermo Scientific Inc., Rockford, IL, USA). Samples were then boiled for 10 min and subjected to SDS-polyacrylamide gel electrophoresis. Proteins were separated and transferred electrophoretically to nitrocellulose membranes (Bio-Rad, Hercules, CA, USA), which were then blocked with 5% bovine serum albumin (BSA) in PBS-T buffer [10 mM phosphate-buffered saline plus 0.05% Tween-20]. Antibodies used to probe the blots were as following: CaV2.3 (1:20,000; Abclonal), teneurin4 (1:1,000; Abcam), CaV1.2 (1:30,000; Alomone Labs), CaV1.3 (1:1,000; Alomone Labs), CUB and sushi domain-containing protein (1:1,000; Abclonal), and GluN2B (1:2,000, Alomone Labs) diluted in PBS-T with 5% skim milk; PKC α (1:2,000, Cell Signaling Technology), adenylyl cyclase type 1 (1:2,000; Abclonal), MeCP2 (1:10,000, Cell Signaling Technology), and β -actin (1:10,000; Abcam) diluted in PBS-T with 5% BSA. Primary antibodies were detected with peroxidase-conjugated secondary antibodies against rabbit IgG (1:2,000; Abcam), mouse IgG (1:5,000; Cell Signaling Technology), or sheep IgG (1:2,000; Abcam) diluted in PBS-T with 5% skim milk, followed by enhanced chemiluminescence (ECL) reagents (Amersham Biosciences, Arlington Heights, IL, USA) and exposure to X-ray film. Band intensities were quantified based on densitometric values using Fujifilm Science Lab 97 Image Gauge software (version 2.54) (Fujifilm, Tokyo, Japan).

Design and procedures

The complete experimental scheme is illustrated in Fig. 1. The number of rats used for different analysis is indicated in Supplementary Fig. 1.

Experiment 1: Two days after the rats were housed separately with two rats per cage, they were serially trained in stages 1 through 6. Once the rats were categorized as either risk-averse or risk-seeking according to the average score of their choices for each window for the last 3 days of stage 6 training, the rats in each group were decapitated 1 day after their final session, and brain tissues (mPFC and NAc) were collected as depicted in Fig. 1. Among a total 34 rats, only those showing clear risk-averse ($n = 9$) or risk-seeking ($n = 10$) preferences were included in the behavioral analysis. To reduce the cost and maximize the contrast between the risk-averse and risk-seeking groups, we excluded intermediate rats ($n = 15$) that were not classified either risk-averse or risk-seeking from the analysis. Due to accidental loss of RNA samples, the final number of rats included in the RNA-seq analysis were nine each for both the risk-averse and risk-seeking groups (Supplementary Table 1).

Experiment 2: The rats were trained and categorized as either risk-averse or risk-seeking in the same manner as in Experiment 1. Subsequently, the rats in each group were

allocated to validation experiments. The rats in each group were decapitated 1 day after their final session, and the brain tissues (mPFC alone) were collected, as depicted in Fig. 1. Out of a total 36 rats, only those showing clear risk-averse ($n = 16$) or risk-seeking ($n = 9$) preferences were included in the subsequent molecular analysis. Intermediate rats ($n = 11$) that were not classified as either risk-averse or risk-seeking were excluded from the analysis. Because of the low quality of the RNA and protein samples, one rat was excluded from each RNA and protein validation analyses. The final number of rats included in the validation analysis was 15 and nine for the risk-averse and risk-seeking groups, respectively. For a validation analysis, we used half sides of the mPFC obtained from the same rats for RT-qPCR and western blot, respectively.

Statistical analysis

The daily choice score data were analyzed with a two-way repeated measure analysis of variance (ANOVA), followed by a Bonferroni *post hoc* test, and the average of the scores on the last 3 days were analyzed using a paired two-tailed Student's *t*-test. The choice-related behavioral parameters were analyzed using an unpaired two-tailed Student's *t*-test. The validation data obtained with RT-qPCR and Western blotting were analyzed using an unpaired two-tailed Student's *t*-test. The correlations between behavioral parameters and the expression levels of the selected genes were examined using the Pearson correlation. The statistical significance was set at a *P*-value of <0.05 .

Ethics

All animal use procedures were conducted according to an approved Institutional Animal Care and Use Committee protocol of Yonsei University College of Medicine.

RESULTS

Risk preference and related behavioral parameters according to the rGT

After the completion of stage 6, rats were clearly divided into risk-averse (advantageous windows, $P1 + P2 \geq 60\%$) and risk-seeking groups (disadvantageous windows, $P3 + P4 \geq 60\%$) (Fig. 2). An ANOVA test conducted on the combined preference choice data obtained from Experiments 1 and 2 showed significant effects of window preference [$F(3,24) = 35.70, P < 0.001$ for risk-averse and $F(3,18) = 7.61, P < 0.001$ for risk-seeking, respectively] and window preference \times day interactions [$F(36,864) = 12.32, P < 0.001$ for risk-averse and $F(36,648) = 9.65, P < 0.001$ for risk-seeking, respectively]. *Post hoc* Bonferroni comparisons revealed that rats in the risk-averse group showed an overwhelming preference for P2 over P4 ($P < 0.001$), which is the most optimal choice, whereas those in the risk-seeking group mostly preferred P4 over P2 ($P < 0.001$), which is the least optimal choice (see the upper right panel in Fig. 1).



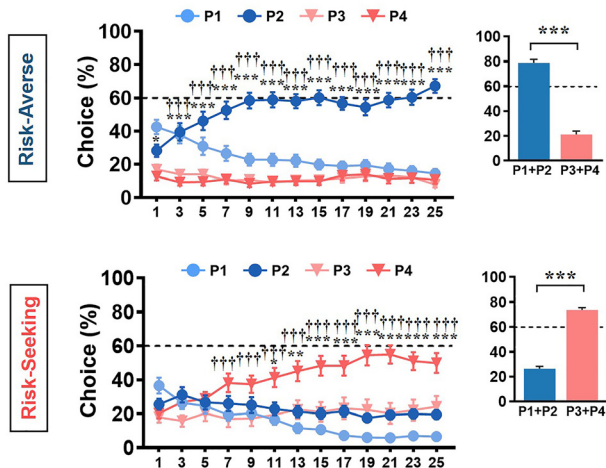


Fig. 2. The combined data obtained during the 25 consecutive days of rGT (stage 6) from Experiments 1 and 2 clearly show different preferences of choice between the groups. The daily window preference choice scores are shown as the percentage of total scores (odd days only; mean \pm S.E.M.); additionally, the average of the last 3 days (mean \pm S.E.M.) for the advantageous (P1+P2) and disadvantageous (P3+P4) scores were shown. The number of rats are 25 and 19 for the risk-averse and risk-seeking groups, respectively

The *t*-test performed on the advantageous and disadvantageous choice scores showed significant effects [$t(24) = 10.82$, $P < 0.001$ for risk-averse and $t(18) = 13.04$, $P < 0.001$ for risk-seeking, respectively]. It was evident that the difference in the choice preference between the two groups was not due to the rats' learning ability, as they showed no distinguishable scores on the accuracy and omission measured during stage 4 (Fig. 3a), indicating that they all passed the learning requirement to move on to the next stages.

We further analyzed several behavioral parameters related to the choice preferences (Cho, Kwak, Kim, & Kim, 2018; van Enkhuizen, Geyer, & Young, 2013; Zeeb et al., 2009) from the data obtained during stage 6. Notably, the risk-seeking group showed significantly higher prematurity scores than the risk-averse group [$t(42) = 2.43$, $P = 0.019$, unpaired *t*-test]. The risk-seeking group also showed significantly lower scores for most of the other parameters: choice latency [$t(42) = 3.90$, $P = 0.0003$], omission [$t(42) = 4.51$, $P < 0.0001$], reward latency [$t(42) = 2.44$, $P = 0.019$], pause after loss timeout [$t(42) = 3.22$, $P = 0.003$], and perseverative responses to all windows or single loss window per 5 s [$t(42) = 2.37$, $P = 0.023$; $t(42) = 2.43$, $P = 0.019$, respectively] (Fig. 3b). These results indicate that the risk-seeking rats were more prone to participating in each trial (low omission), with a significant tendency of faster responses to the results of present choice (low scores for reward latency, pause after loss timeout, and perseverative responses) and to the next trial (low choice latency and high prematurity).

Transcriptome profiles contributing to the expression of risky choice

To identify the transcriptional components underlying risky choices, we targeted two brain regions, the mPFC and the

NAC, which are known to play an important role in decision-making and addictive disorders (de Visser, Baars, et al., 2011; Fellows & Farah, 2005; Goto & Grace, 2008; Kim et al., 2013; Orsini et al., 2018). We performed WTS on the brain samples obtained from the rGT rats (Fig. 1). We defined DEGs by a *q*-value of <0.1 and 1.3 times of fold change, and identified 477 and 36 DEGs in the mPFC and the NAC respectively, between the two groups (Fig. 4 and 5a, and Supplementary Table 3 for the whole lists). Unsupervised hierarchical clustering analyses of the DEGs in the NAC revealed a distinct pattern between the two groups, with two exceptions (Fig. 4a middle), whereas those in the mPFC completely separated the two groups (Fig. 4b middle). The numbers of uniquely detected DEGs in the mPFC and the NAC was 458 and 17, respectively (Fig. 5a). Among these, well-known addiction-related genes, including *Grin2a*, *Grin2b*, *Prkca*, and *Cacna1d* (Cornelis et al., 2016; Martinez-Rivera et al., 2017; Caffino et al., 2019), were downregulated in the mPFC (see Supplementary Table 3 for the full lists).

Subsequently, we performed GO- and pathway-level functional enrichment analysis using Metascape (Zhou et al., 2019) and found that most of the enriched clusters were identified in the downregulated genes in the mPFC (Fig. 5b). Notably, downregulated genes in the mPFC were significantly enriched in terms related to glutamatergic synapse, chemical synaptic transmission, associative learning, and addiction. Some examples of gene descriptions were glutamatergic synapse ($P = 1.5 \times 10^{-15}$), calcium signaling pathway ($P = 1.2 \times 10^{-12}$), synaptic signaling ($P = 1.9 \times 10^{-7}$), behavior ($P = 6.5 \times 10^{-9}$), cognition ($P = 2.2 \times 10^{-8}$), nicotine addiction ($P = 4.6 \times 10^{-4}$), and amphetamine addiction ($P = 8.4 \times 10^{-4}$) (Fig. 5b and Supplementary Table 4 for the full lists). Notably, among the downregulated genes, 19 genes shared by the mPFC and the NAC were significantly enriched only in a cluster representing metal ion transmembrane transporter activity (GO:0046873), where *Cacna1e* (voltage-dependent Ca^{2+} channel) and *Slc4a8* (Na^+ - driven $\text{Cl}^-/\text{HCO}_3^-$ exchanger) were included (Saegusa et al., 2000; Sinning et al., 2011) (Fig. 5a and b). These results imply that the genes in these clusters are more likely to be involved in the process of promoting risky choices in rGT.

To further identify closely related genes, we performed a PPI network analysis of 358 downregulated genes in the mPFC (Fig. 4b) using the MCODE algorithm (Bader & Hogue, 2003), which revealed 72 genes as densely connected with seven MCODE networks (Fig. 5c and Supplementary Table 5). Among them, approximately 80% of the genes appeared to be associated with MCODE1-3, suggesting that they were more likely to be related to the phenotype of risk-seeking behavior. It is notable that MCODE1 (25 genes) was significantly enriched, for example, in the voltage-gated calcium channel complex (GO:0005891), dopaminergic synapse (rno04728), cognition (GO:0050890), and behavior (GO:0007610), while MCODE2 (17 genes) showed NMDA glutamate receptor activity (GO:0004972), nicotine/cocaine/amphetamine addiction (rno05033/rno05030/rno05031), and long-term potentiation (rno04720). Similarly, MCODE3



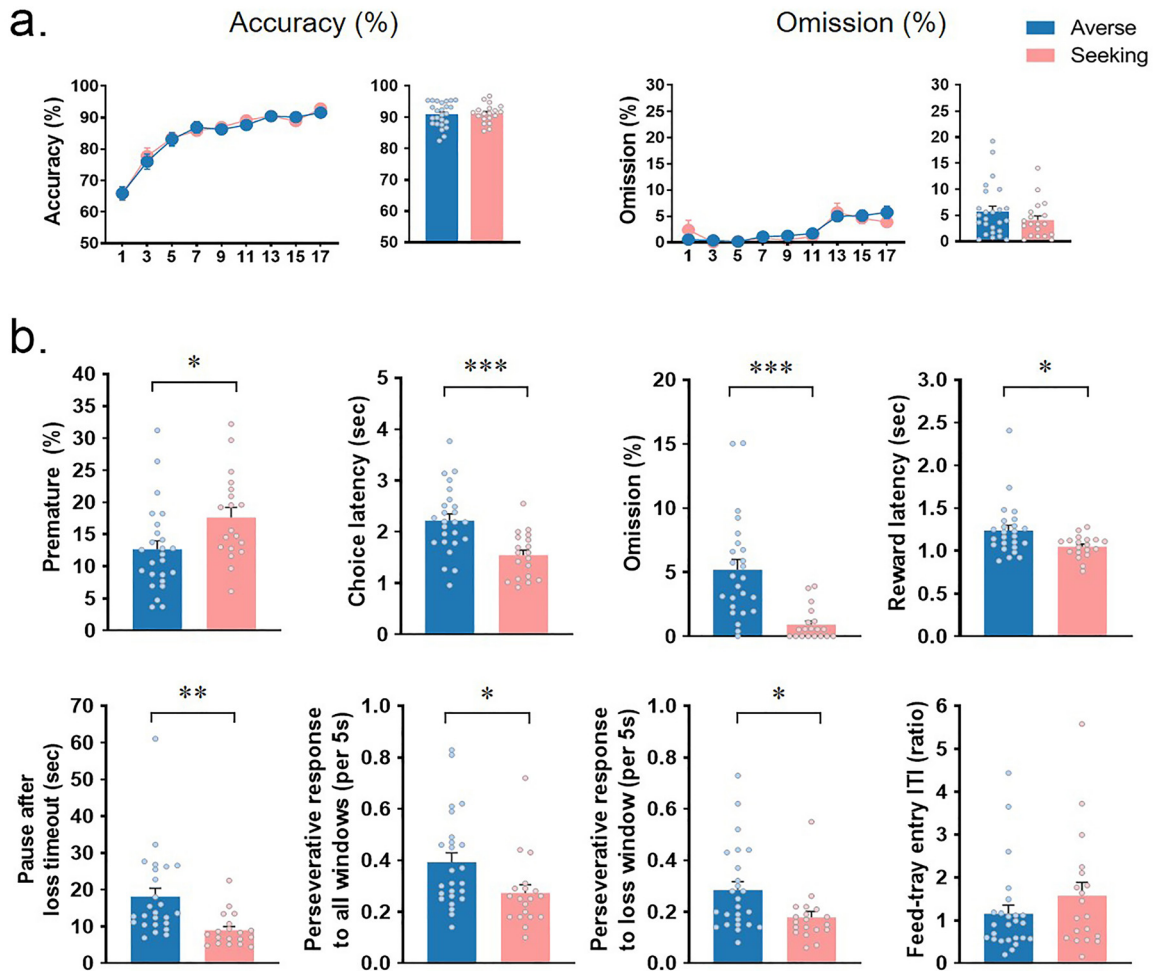


Fig. 3. Analysis of behavioral parameters between the risk-averse and risk-seeking groups. (a) The accuracy and omission were measured as percentage during 5-CSRTT training (Stage 4). In each panel, the results of the daily sessions for 17 days (left, odd days only) and the average of the last 3 days (right) are shown. By the end of the training, all the rats in each group fulfilled the final criteria (accuracy >80% and omission <20%). The number of rats are 25 and 19 for the risk-averse and risk-seeking groups, respectively. (b) The average scores of the last 3 day-measurements (Stage 6) of choice-related behavioral parameters between the risk-averse and risk-seeking groups are shown. Data are shown as mean + S.E.M. *** $P < 0.001$, ** $P < 0.01$, * $P < 0.05$

(15 genes) was significantly enriched in glutamatergic synapse (rno04724), learning or memory (GO:0007611), and cognition (GO:0050890).

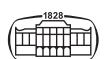
Validation of DEGs in the mPFC

To validate the downregulated genes identified in the mPFC in the risk-seeking group compared to the risk-averse group, we selected the top three genes based on their significance level (*Csmd2*, *Cacna1e*, and *Tenm4*) and six additional genes (*Cacna1c*, *Cacna1d*, *Prkca*, *Adcy1*, *Grin2b*, and *MeCP2*) from the GO terms that we thought might be interesting to examine in terms of synaptic transmission and signalling pathways. An RT-qPCR analysis of the RNA samples obtained from an independent replication set of rGT trained rats (Fig. 1) revealed that five genes (*Cacna1e*, *Tenm4*, *Cacna1c*, *Cacna1d*, and *Prkca*) were significantly downregulated in the risk-seeking group compared with the risk-averse group, consistent with RNA-seq results (Fig. 6a). The other four genes were also downregulated in the risk-seeking

group but did not reach significant levels. We further validated these genes by Western blotting and revealed that two genes (*Cacna1e* and *Tenm4*) were also significantly downregulated in the risk-seeking group compared to the risk-averse group. This was consistent with RNA-seq and RT-qPCR results (Fig. 6b).

Correlation analysis between choice-related behaviors and down-regulated genes in the mPFC

To examine whether five genes (*Cacna1e*, *Tenm4*, *Cacna1c*, *Cacna1d*, and *Prkca*), which appeared statistically significant after validation by RT-qPCR and western analysis, were correlated with some choice-related behaviors (see Figs 2 and 3), we conducted a Pearson correlation analysis on the data obtained from rats with three different levels of gene analysis (RNA-seq, RT-qPCR, and western). When we examined the choice preference data, it was found that there were significant correlations between the RNA-seq values and the individual choice preference scores for all five genes



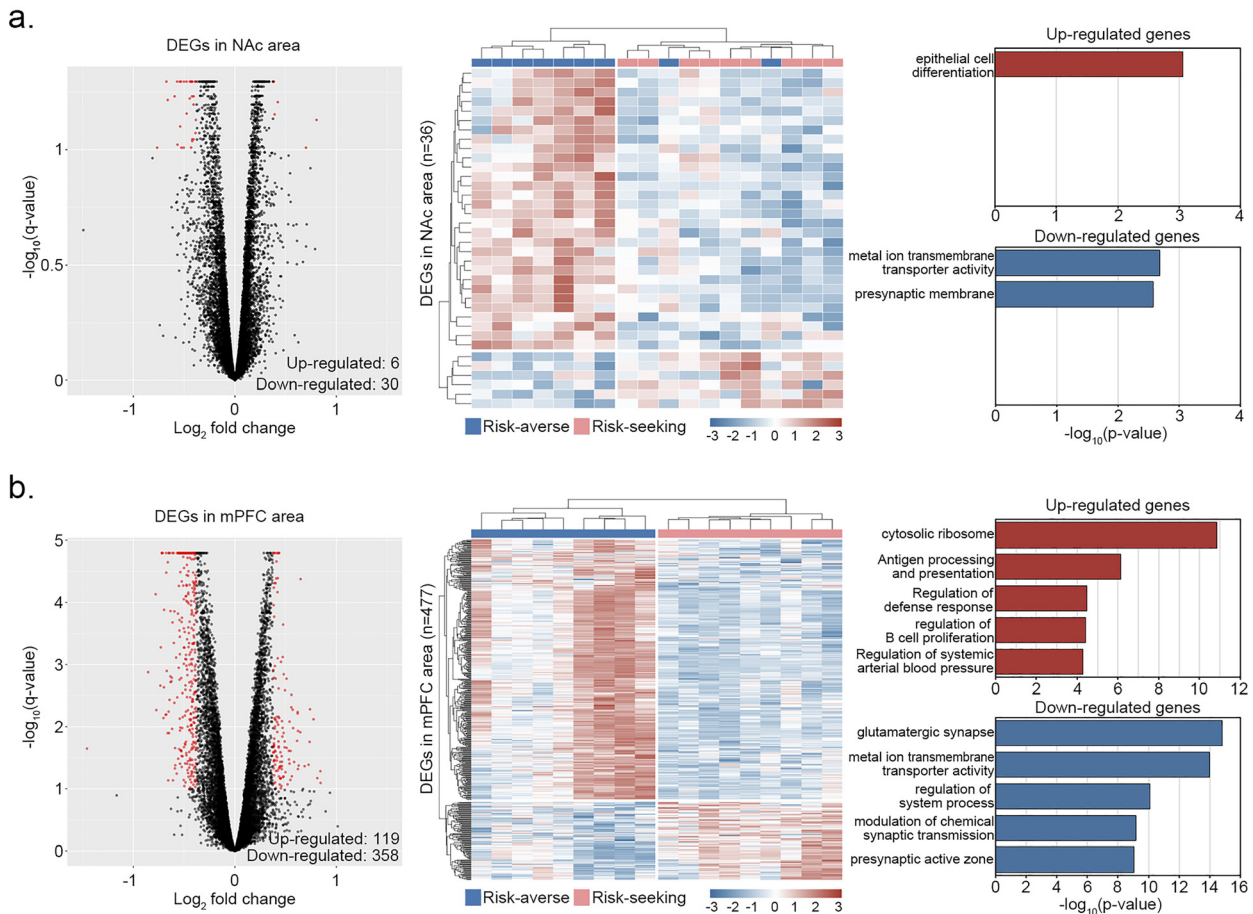


Fig. 4. Transcriptome profiles contributing to the expression of risky choice. (a, b) Red dots in the volcano plot (left) indicate DEGs in the risk-seeking group against those of the risk-averse group with values of \log_2 fold change >0.38 and q -value of <0.1 . The complete lists and details of the DEGs are available in Supplementary Table 3. The middle panel represents the unsupervised hierarchical clustering of DEGs in the two brain regions. Reds and blues indicate up-regulated and down-regulated genes, respectively. The top five statistically enriched terms from GO or KEGG pathways for up-regulated (red) and down-regulated (blue) genes are shown (right). The number of rats are 9 each for both the risk-averse and risk-seeking groups

(Supplementary Table 6). In addition, there were significant correlations between the RT-qPCR values and choice scores (P2, P4) in *Cacna1d* ($r = -0.48$, $P = 0.018$ and $r = -0.46$, $P = 0.025$, respectively), whereas there was a significant negative correlation between the western blot values and choice scores (P4) in *Cav2.3* (*Cacna1e*) ($r = -0.52$, $P = 0.01$) (Supplementary Figure 2).

When we examined the choice-related behavioral parameter data, we found that there were significant positive correlations between the RNA-seq values and omission scores in all five genes ($r = 0.48$ – 0.59 , $P = 0.044$ – 0.01). However, there was only a significant positive correlation between the RT-qPCR values and perseverative response to the loss window scores in *Cacna1d* ($r = 0.41$, $P = 0.049$) (Supplementary Figure 3).

DISCUSSION

This study investigated DEGs in two brain regions (the mPFC and the NAc) between risk-averse and risk-seeking

groups of rGT-trained rats using whole-transcriptome analysis. We determined that 358 genes (approximately 75% of the total differentially expressed genes) were down-regulated in the mPFC of risk-seeking rats compared to risk-averse rats, which suggests a transcriptional component of neuronal mechanisms underlying risky choices in rats.

A whole-transcriptome analysis of the brain regions of rGT rats revealed that the number of uniquely detected DEGs in the mPFC was 27 times higher than that in the NAc (458 versus 17, Fig. 5a), suggesting that the mPFC may contribute more significantly to the expression of risky choices than the NAc. Notably, GO- and pathway-level functional enrichment analyses and additional PPI network analysis of 358 downregulated genes in the mPFC revealed 72 genes that were densely connected with seven MCODE networks (Fig. 5c). Among them, 57 genes in the MCODE1~3 and 4 genes in the MCODE5 networks were found to be significantly enriched in the voltage-gated calcium channel complex, voltage-gated potassium channel complex, dopaminergic synapse, glutamatergic synapse, behavior, addictions, and cognition, suggesting that they are



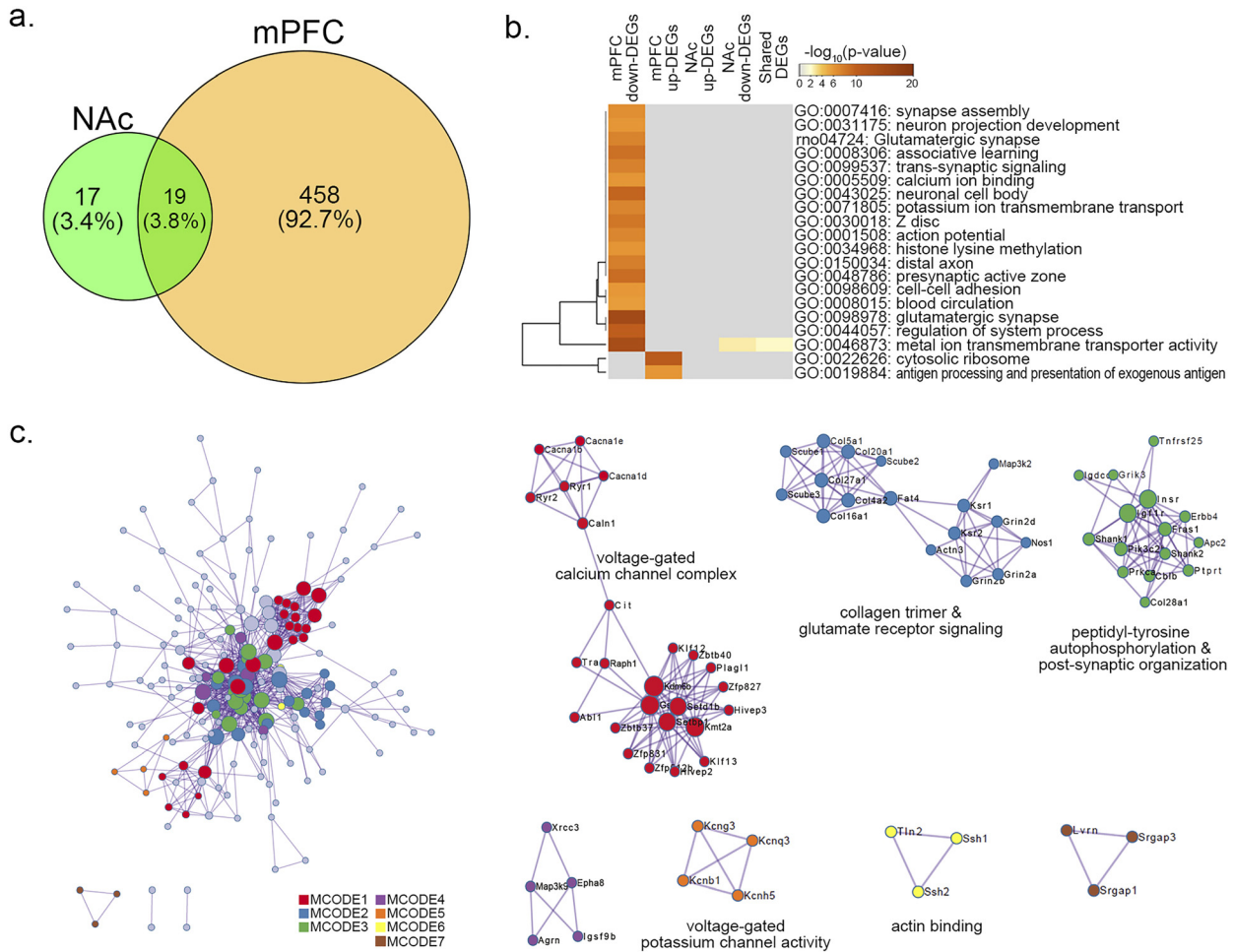


Fig. 5. (a) The Venn diagram shows the number of DEGs uniquely detected in the two brain regions, resulting in about 27 times higher in the mPFC than in the NAc. (b) Heatmap shows the top 20 enriched ontology clusters for up-regulated, down-regulated, and shared genes in the two brain regions using a discrete color scale to represent the different statistical significances. The best nominal *P*-value within each cluster was selected as its representative term and displayed in a dendrogram. Most of the enriched clusters were identified in down-regulated genes in the mPFC. The complete lists and details of these data with *q*-values are available in Supplementary Table 4. (c) PPI network for down-regulated genes in the mPFC. Each dot represents a down-regulated target gene. The hub-gene groups identified by the MCODE algorithm were labeled as MCODE 1–7 with a unique color allotted to each of them. GO and KEGG pathway enrichment analyses were applied to each MCODE component independently, and the best-scoring terms by *P*-value were retained as the functional description of the corresponding components. The complete lists and details of these data with *q*-values are available in Supplementary Table 5. The number of rats are 9 each for both the risk-averse and risk-seeking groups, respectively

commonly involved in the regulation of synaptic plasticity related to decision-making. For example, dopamine and glutamate are well known for their roles in associative learning and reward processes related to addiction and decision-making (Gardoni & Bellone, 2015; Mascia et al., 2020; Schultz, 2011). Thus, it will be of great interest to examine how manipulation of these genes affects the outcomes of risk-choice behavior in the future. Other MCODE networks (4, 6, 7) were not identified in our initial functional enrichment analysis, and they do not seem directly related to the neuronal processes underlying risky choices; they only remained for their possible functional roles to be investigated in the future.

Subsequent validation analyses by RT-qPCR revealed that five genes (*Cacna1e*, *Tenm4*, *Cacna1c*, *Cacna1d*, and *Prkca*) were significantly downregulated in the risk-seeking

group compared with the risk-averse group (Fig. 6a). Here, we should acknowledge that, in addition to the top three genes based on their significance level (*Csmd2*, *Cacna1e*, and *Tenm4*), we arbitrarily chose six genes (*Cacna1c*, *Cacna1d*, *Prkca*, *Adcy1*, *Grin2b*, and *MeCP2*) that we presumed might be significant to examine. These results suggest that the ranks of the individual genes based on their significance levels by an RNA-seq analysis do not necessarily match the validation results. As we found significant downregulation in some arbitrarily selected genes, there could be additional genes showing significantly differential expression out of the 458 genes uniquely detected in the mPFC (Fig. 5a), which remain to be explored in the future. Further validation analyses by Western blot analysis revealed that two genes (*Cacna1e* and *Tenm4*) were significantly downregulated in the risk-seeking group compared to the risk-averse group



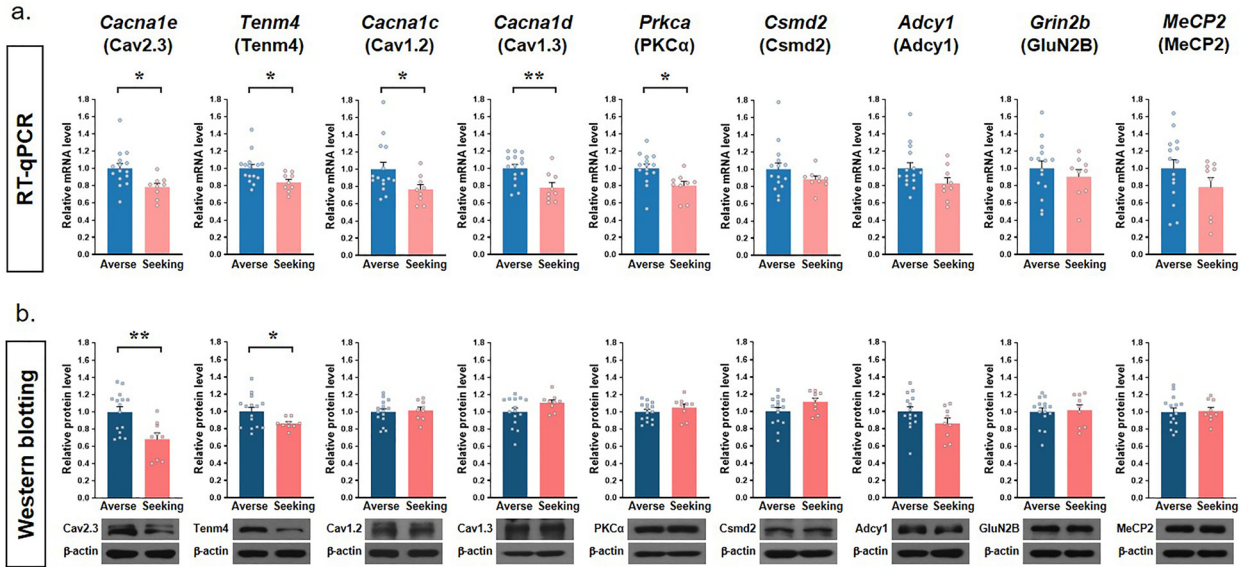


Fig. 6. Validation for the down-regulation of genes in risk-seeking rats. The validation experiment detected significant reductions in the expression levels for a few genes by RT-qPCR (a) and further by western blot (b), similar to the findings in RNA-seq analysis. The values are mean + S.E.M. of relative expression of molecules in the risk-seeking group compared to the risk-averse group. * $P < 0.05$, ** $P < 0.01$, risk-seeking compared to risk-averse. The number of rats are 15 and 9 for the risk-averse and risk-seeking group, respectively

(Fig. 6b). *Cacna1e* encodes an alpha 1E subunit, known as CaV2.3, of the R-type calcium channel, which is a voltage-dependent calcium channel located in the dendritic spines with strong expression in the cortex, striatum, amygdala, and hippocampus (Parajuli et al., 2012). The CaV2.3 channels are known to be involved in diverse functions, such as spatial memory (Kubota et al., 2001), synaptic plasticity (Breustedt, Vogt, Miller, Nicoll, & Schmitz, 2003), morphine analgesia and tolerance (Yokoyama et al., 2004), fear memory (Zhang et al., 2016), and the regulation of dopamine loss related to Parkinson's disease (Benkert et al., 2019). On the other hand, *Tenm4* encodes teneurin-4, a transmembrane protein highly expressed in the central nervous system. Relatively little is known about its functional roles, although teneurin-4 has been reported to play a role in establishing proper neuronal connectivity during development and differentiation (Suzuki et al., 2012, 2014), and in the etiology of schizophrenia (Xue et al., 2019). Considering their functional roles, the down-regulation of these genes in the mPFC implies that they may have influenced synaptic connectivity and subsequent plastic changes in this brain region, eventually leading to the expression of characteristic risky choice behavior in the risk-seeking group.

Correlation analyses between five validated genes (*Cacna1e*, *Tenm4*, *Cacna1c*, *Cacna1d*, and *Prkca*) (Fig. 6a) and choice preference scores (Fig. 2) revealed significant correlations between the gene expression levels and choice scores in all five genes by RNA-seq (Supplementary Table 6), only in *Cacna1d* by RT-qPCR and Cav2.3 (*Cacna1e*) by western blot analysis (Supplementary Fig. 2). Furthermore, correlation analyses between these genes and choice-related

behavioral parameters (Fig. 3) revealed significant positive correlations between the gene expression levels and omission scores in all five genes measured by RNA-seq, whereas there was only a significant positive correlation between the gene expression levels and perseverative response to the loss window scores in *Cacna1d* measured by RT-qPCR (Supplementary Fig. 3). These results imply that the behavioral output, manifested as choice preference in our case, cannot be attributed to any single gene; rather, it is influenced by the sum of a few or several genes. Considering that behavior, especially when accompanied by a higher level of cognitive function, is a complicated phenotype, it is not surprising that several genes are involved simultaneously or sequentially at different levels of expression (i.e., transcriptome, mRNA, protein, etc). In line with this consideration, although some significant correlations that we found may suggest that those genes could contribute more strongly to choice behavior, caution should be exerted when applying these data for whole interpretation.

It is worth mentioning that naïve rats (not rGT-trained) were not included in our present analyses because we wanted to focus solely on identifying DEGs between the same rGT trained but differently categorized rats according to their traits, rather than to focus on finding differences in rGT itself from naïve rats. Furthermore, our data are limited to Sprague-Dawley rats that we used in the present study, leaving other rat strains that may be more or less vulnerable to addictive behaviors unresolved. Regarding the brain regions, although we detected overwhelming levels of changes in the gene expression in the mPFC, distinguishing the two groups, these results cannot completely exclude any possible important roles of the NAc in making risky choices.

Small but critical genes, if any, may reside in the NAc, and should be investigated in the future. Moreover, the cell types in these regions that play pivotal roles need to be investigated. As it is a common limitation of whole-transcriptome sequencing, which uses bulk-tissue, we may attempt an in-depth investigation at the single-cell level resolution, using the recent development of single-cell RNA sequencing or spatial gene expression technologies (Joglekar et al., 2021; Maynard et al., 2021; Ren et al., 2019; Tiklová et al., 2019), to obtain cell type information related to risk preference and thereby useful biomarkers in the future. Finally, to expand our present findings, a comparison of genes regulated by the rGT with those that appeared dysregulated in psychiatric conditions revealed by human genome-wide association studies or other omics studies, such as epigenomics and proteomics, will definitely help us to understand the molecular pathogenesis of decision-making and related psychiatric conditions.

CONCLUSION

To the best of our knowledge, this is the first study to conduct whole-transcriptome analysis of the brain regions of rGT rats. Our findings revealed significantly downregulated genes and their clusters in the mPFC in risk-seeking rats compared to those in risk-averse rats. Considering that the rGT uses rats as subjects, it has unique advantages in finding the behavioral and molecular mechanisms that underlie the complexity of choice behavior by allowing the intentional interference and manipulation of the experimenter. Thus, the present findings will be useful for providing insights into challenging future scenarios.

Funding sources: This work was supported by the Brain Research Program (2014M3C7A1062895, 2015M3C7A1064778), the Mid-Career Researcher Programs (2019R1A2C1011262, 2019R1A2C2089518), Young Researcher Program (2019R1C1C1004909), Medical Research Center (2019R1A5A2027588), and Korea Post-Genome Project (2017M3C9A6047615) through the National Research Foundation of Korea funded by the Ministry of Science and ICT.

Authors' contribution: WYK and JHK conceived the project and designed the experiments. MJK, WYK and JHK designed the strategy for animal experiments. MJK and WYK performed the animal experiments. SHJ and YJC designed and performed transcriptome analysis. WYK, SHJ and JHK wrote the paper. MJK and SHJ prepared the figures. All authors approved the final version of the manuscript.

Conflict of interest: The authors declare no conflicts of interest.

Acknowledgments: We thank Medical Illustration & Design, a part of the Medical Research Support Services at Yonsei University College of Medicine, for providing artistic support with schematic illustration.

SUPPLEMENTARY MATERIAL

Supplementary data to this article can be found online at <https://doi.org/10.1556/2006.2022.00068>.

REFERENCES

- Anders, S., Pyl, P. T., & Huber, W. (2015). HTSeq—a Python framework to work with high-throughput sequencing data. *Bioinformatics*, *31*, 166–169. <https://doi.org/10.1093/bioinformatics/btu638>.
- Anokhin, A. P., Golosheykin, S., Grant, J., & Heath, A. C. (2009). Heritability of risk-taking in adolescence: A longitudinal twin study. *Twin Research and Human Genetics*, *12*, 366–371. <https://doi.org/10.1375/twin.12.4.366>.
- Baarendse, P. J., Winstanley, C. A., & Vanderschuren, L. J. (2013). Simultaneous blockade of dopamine and noradrenaline reuptake promotes disadvantageous decision making in a rat gambling task. *Psychopharmacology*, *225*, 719–731. <https://doi.org/10.1007/s00213-012-2857-z>.
- Bader, G. D., & Hogue, C. W. (2003). An automated method for finding molecular complexes in large protein interaction networks. *BMC Bioinformatics*, *4*, 2. <https://doi.org/10.1186/1471-2105-4-2>.
- Bechara, A. (2003). Risky business: Emotion, decision-making, and addiction. *Journal of Gambling Studies*, *2003*, 23–51. <https://doi.org/10.1023/a:1021223113233>.
- Bechara, A., Damasio, A. R., Damasio, H., & Anderson, S. W. (1994). Insensitivity to future consequences following damage to human prefrontal cortex. *Cognition*, *50*, 7–15. [https://doi.org/10.1016/0010-0277\(94\)90018-3](https://doi.org/10.1016/0010-0277(94)90018-3).
- Benkert, J., Hess, S., Roy, S., Beccano-Kelly, D., Wiederspohn, N., Duda, J., ... Liss, B. (2019). CaV2.3 channels contribute to dopaminergic neuron loss in a model of Parkinson's disease. *Nature Communications*, *10*, 5094. <https://doi.org/10.1038/s41467-019-12834-x>.
- Black, D. W., Monahan, P. O., Temkit, M., & Shaw, M. (2006). A family study of pathological gambling. *Psychiatry Research*, *141*, 295–303. <https://doi.org/10.1016/j.psychres.2005.12.005>.
- Bolger, A. M., Lohse, M., & Usadel, B. (2014). Trimmomatic: A flexible trimmer for Illumina sequence data. *Bioinformatics*, *30*, 2114–2120. <https://doi.org/10.1093/bioinformatics/btu170>.
- Breustedt, J., Vogt, K. E., Miller, R. J., Nicoll, R. A., & Schmitz, D. (2003). Alpha 1E-containing Ca²⁺ channels are involved in synaptic plasticity. *Proceedings of the National Academy of Sciences of the United States of America*, *100*, 12450–12455. <https://doi.org/10.1073/pnas.2035117100>.
- Caffino, L., Verheij, M. M. M., Que, L., Guo, C., Homberg, J. R., & Fumagalli, F. (2019). Increased cocaine self-administration in rats lacking the serotonin transporter: A role for glutamatergic signaling in the habenula. *Addiction Biology*, *24*, 1167–1178. <https://doi.org/10.1111/adb.12673>.
- Cardinal, R. N., & Aitken, M. R. (2010). Whisker: A client-server high-performance multimedia research control system. *Behavioural Research Methods*, *42*, 1059–1071. <https://doi.org/10.3758/brm.42.4.1059>.



- Cho, B. R., Kwak, M. J., Kim, W. Y., & Kim, J.-H. (2018). Impulsive action and impulsive choice are differentially expressed in rats depending on the age at exposure to an ambling task. *Frontiers in Psychiatry*, 9, 503. <https://doi.org/10.3389/fpsy.2018.00503>.
- Cornelis, M. C., Flint, A., Field, A. E., Kraft, P., Han, J., Rimm, E. B., & van Dam, R. M. (2016). A genome-wide investigation of food addiction. *Obesity*, 24, 1336–1341. <https://doi.org/10.1002/oby.21476>.
- de Visser, L., Baars, A. M., van't Klooster, J., & van den Bos, J. R. (2011). Transient inactivation of the medial prefrontal cortex affects both anxiety and decision-making in male Wistar rats. *Frontiers in Neuroscience*, 5, 102. <https://doi.org/10.3389/fnins.2011.00102>.
- de Visser, L., Homberg, J. R., Mitsogiannis, M., Zeeb, F. D., Rivalan, M., & Fitoussi, A. (2011). Rodent versions of the Iowa gambling task: Opportunities and challenges for the understanding of decision-making. *Frontiers in Neuroscience*, 5, 109. <https://doi.org/10.3389/fnins.2011.00109>.
- Dobin, A., Davis, C. A., Schlesinger, F., Drenkow, J., Zaleski, C., Jha, S., ... Gingeras, T. R. (2013). STAR: Ultrafast universal RNA-seq aligner. *Bioinformatics*, 29, 15–21. <https://doi.org/10.1093/bioinformatics/bts635>.
- Ducci, F., & Goldman, D. (2012). The genetic basis of addictive disorders. *The Psychiatric Clinics of North America*, 35, 495–519. <https://doi.org/10.1093/med/9780199934959.003.0052>.
- Fauth-Bühler, M., Mann, K., & Potenza, M. N. (2017). Pathological gambling: A review of the neurobiological evidence relevant for its classification as an addictive disorder. *Addiction Biology*, 22, 885–897. <https://doi.org/10.1111/adb.12378>.
- Fellows, L. K., & Farah, M. J. (2005). Different underlying impairments in decision-making following ventromedial and dorsolateral frontal lobe damage in humans. *Cerebral Cortex*, 15, 58–63. <https://doi.org/10.1111/adb.12378>.
- Frascella, J., Potenza, M. N., Brown, L. L., & Childress, A. R. (2010). Shared brain vulnerabilities open the way for nonsubstance addictions: Craving addiction at a new joint? *Annals of the New York Academy of Sciences*, 1187, 294–315. <https://doi.org/10.1111/j.1749-6632.2009.05420.x>.
- Gardoni, F., & Bellone, F. C. (2015). Modulation of the glutamatergic transmission by dopamine: A focus on Parkinson, huntington and addiction diseases. *Frontiers in Cellular Neuroscience*, 9, 25. <https://doi.org/10.3389/fncel.2015.00025>.
- Goto, Y., & Grace, A. A. (2008). Limbic and cortical information processing in the nucleus accumbens. *Trends in Neurosciences*, 31, 552–558. <https://doi.org/10.1016/j.tins.2008.08.002>.
- Huggett, S. B., & Stallings, M. C. (2020). Cocaine'omics: Genome-wide and transcriptome-wide analyses provide biological insights into cocaine use and dependence. *Addiction Biology*, 25, e12719. <https://doi.org/10.1111/adb.12719>.
- Joglekar, A., Pribelski, A., Mahfouz, A., Collier, P., Lin, S., Schlusche, A. K., ... Tilgner, H. U. (2021). A spatially resolved brain region- and cell type-specific isoform atlas of the postnatal mouse brain. *Nature Communications*, 12, 463. <https://doi.org/10.1038/s41467-020-20343-5>.
- Jung, S. H., Yim, S. H., Hu, H. J., Lee, K. H., Lee, J. H., Sheen, D. H., ... Chung, Y. J. (2014). Genome-wide copy number variation analysis identifies deletion variants associated with ankylosing spondylitis. *Arthritis & Rheumatology*, 66, 2103–2112. <https://doi.org/10.1002/art.38650>.
- Kim, W. Y., Cho, B. R., Kwak, M. J., & Kim, J.-H. (2017). Interaction between trait and housing condition produces differential decision-making toward risk choice in a rat gambling task. *Scientific Reports*, 7, 5718. <https://doi.org/10.1038/s41598-017-06408-4>.
- Kim, W. Y., Jang, J. K., Lee, J. W., Jang, H., & Kim, J.-H. (2013). Decrease of GSK3 β phosphorylation in the rat nucleus accumbens core enhances cocaine-induced hyper-locomotor activity. *Journal of Neurochemistry*, 125, 642–648. <https://doi.org/10.1111/jnc.12222>.
- Kubota, M., Murakoshi, T., Saegusa, H., Kazuno, A., Zong, S., Hu, Q., ... Tanabe, T. (2001). Intact LTP and fear memory but impaired spatial memory in mice lacking CaV2.3 (alpha 1E) channel. *Biochemical and Biophysical Research Communications*, 282, 242–248. <https://doi.org/10.1006/bbrc.2001.4572>.
- Lang, M., Leménager, T., Streit, F., Fauth-Bühler, M., Frank, J., Juraeva, D., ... Mann, K. F. (2020). Genome-wide association study of pathological gambling. *European Psychiatry*, 36, 38–46. <https://doi.org/10.1016/j.eurpsy.2016.04.001>.
- Lind, P. A., Zhu, G., Montgomery, G. W., Madden, P. A. F., Heath, A. C., Martin, N. G., & Slutske, W. S. (2012). Genome-wide association study of a quantitative disordered gambling trait. *Addiction Biology*, 18, 511–522. <https://doi.org/10.1111/j.1369-1600.2012.00463.x>.
- Lobo, D. S. S., Aleksandrova, L., Knight, J., Casey, D. M., el-Guebaly, N., Nobrega, J. N., & Kennedy, J. L. (2015). Addiction-related genes in gambling disorders: New insights from parallel human and pre-clinical models. *Molecular Psychiatry*, 20, 1002–1010. <https://doi.org/10.1038/mp.2014.113>.
- Lobo, D. S. S., & Kennedy, J. L. (2009). Genetic aspects of pathological gambling: A complex disorder with shared genetic vulnerabilities. *Addiction*, 104, 1454–1465. <https://doi.org/10.1111/j.1360-0443.2009.02671.x>.
- Mar, A. C., Horner, A. E., Nilsson, S. R. O., Alsiö, J., Kent, B. A., Kim, C. H., ... Bussey, T. J. (2013). The touchscreen operant platform for assessing executive function in rats and mice. *Nature Protocols*, 8, 1985–2005. <https://doi.org/10.1038/nprot.2013.123>.
- Martinez-Rivera, A., Hao, J., Tropea, T. F., Giordano, T. P., Kosovsky, M., Rice, R. C., ... Rajadhyaksha, A. M. (2017). Enhancing VTA Ca_v1.3 L-type Ca²⁺ channel activity promotes cocaine and mood-related behaviors via overlapping AMPA receptor mechanisms in the nucleus accumbens. *Molecular Psychiatry*, 22, 1735–1745. <https://doi.org/10.1038/mp.2017>.
- Mascia, P., Wang, Q., Brown, J., Nesbitt, K. M., Kennedy, R. T., & Vezina, P. (2020). Maladaptive consequences of repeated intermittent exposure to uncertainty. *Progress in Neuro-psychopharmacology & Biological Psychiatry*, 99, 109864. <https://doi.org/10.1016/j.pnpbp.2020.109864>.
- Maynard, K. R., Collado-Torres, L., Weber, L. M., Uyttingco, C., Barry, B. K., Williams, S. R., ... Jaffe, A. E. (2021). Transcriptome-scale spatial gene expression in the human dorso-lateral prefrontal cortex. *Nature Neuroscience*, 24, 425–436. <https://doi.org/10.1038/s41593-020-00787-0>.
- Navandar, M., Martin-Garcia, E., Maldonado, R., Lutz, B., Gerber, S., & Azua, I. R. (2021). Transcriptional signatures in prefrontal



- cortex confer vulnerability versus resilience to food and cocaine addiction-like behavior. *Scientific Reports*, 11, 9076. <https://doi.org/10.1038/s41598-021-88363-9>.
- Orsini, C. A., Heshmati, S. C., Garman, T. S., Wall, S. C., Bizon, J. L., & Setlow, B. (2018). Contributions of medial prefrontal cortex to decision making involving risk of punishment. *Neuropharmacology*, 139, 205–216. <https://doi.org/10.1016/j.neuropharm.2018.07.018>.
- Parajuli, L. K., Nakajima, C., Kulik, A., Matsui, K., Schneider, T., & Shigemoto, R., & Fukazawa, Y. (2012). Quantitative regional and ultrastructural localization of the CaV2.3 subunit of T-type calcium channel in mouse brain. *Journal of Neuroscience*, 32, 13555–13567. <https://doi.org/10.1523/jneurosci.1142-12.2012>.
- Piasecki, T. M., Gizer, I. R., & Slutske, W. S. (2019). Polygenic risk scores for psychiatric disorders reveal novel clues about the genetics of disordered gambling. *Twin Research and Human Genetics*, 22, 283–289. <https://doi.org/10.1017/thg.2019.90>.
- Potenza, M. N. (2008). The neurobiology of pathological gambling and drug addiction: An overview and new findings. *Philosophical Transactions of The Royal Society B*, 363, 3181–3189. <https://doi.org/10.1098/rstb.2008.0100>.
- Potenza, M. N. (2009). The importance of animal models of decision making, gambling, and related behaviors: Implications for translational research in addiction. *Neuropsychopharmacology*, 34, 2623–2624. <https://doi.org/10.1038/npp.2009.152>.
- Ren, J., Isakova, A., Friedmann, D., Zeng, J., Grutzner, S. M., Pun, A., ... Luo, L. (2019). Single-cell transcriptomes and whole-brain projections of serotonin neurons in the mouse dorsal and median raphe nuclei. *eLife*, 8, e49424. <https://doi.org/10.7554/elife.49424>.
- Rivalan, M., Ahmed, S. H., & Dellu-Hagedorn, F. (2009). Risk-prone individuals prefer the wrong options on a rat version of the Iowa gambling task. *Biological Psychiatry*, 66, 743–749. <https://doi.org/10.1016/j.biopsych.2009.04.008>.
- Robinson, M. D., McCarthy, D. J., & Smyth, G. K. (2010). edgeR: a Bioconductor package for differential expression analysis of digital gene expression data. *Bioinformatics*, 26, 139–140. <https://doi.org/10.1093/bioinformatics/btp616>.
- Saegusa, H., Kurihara, T., Zong, S., Minowa, O., Kazuno, A., Han, W., ... Tanabe, T. (2000). Altered pain responses in mice lacking alpha 1E subunit of voltage-dependent Ca²⁺ channel. *Proceedings of the National Academy of Sciences of the United States of America*, 97, 6132–6137. <https://doi.org/10.1073/pnas.100124197>.
- Schultz, W. (2011). Potential vulnerabilities of neuronal reward, risk, and decision mechanisms to addictive drugs. *Neuron*, 69, 603–617. <https://doi.org/10.1016/j.neuron.2011.02.014>.
- Sinning, A., Liebmann, L., Kougioumtzes, A., Westermann, M., Bruehl, C., & Hübner, C. A. (2011). Synaptic glutamate release is modulated by the Na⁺-driven Cl⁻/HCO₃⁻ exchanger Slc_{4a8}. *Journal of Neuroscience*, 31, 7300–7311. <https://doi.org/10.1523/jneurosci.0269-11.2011>.
- Slutske, W. S., Eisen, S., True, W. R., Lyons, M. J., Goldberg, J., & Tsuang, M. (2000). Common genetic vulnerability for pathological gambling and alcohol dependence in men. *Archives of General Psychiatry*, 57, 666–673. <https://doi.org/10.1001/archpsyc.57.7.666>.
- Suzuki, N., Fukushi, M., Kosaki, K., Doyle, A. D., de Vega, S., & Yoshizaki, K., ... Yamada, Y. (2012). Teneurin-4 is a novel regulator of oligodendrocyte differentiation and myelination of small-diameter axons in the CNS. *Journal of Neuroscience*, 32, 11586–11599. <https://doi.org/10.1523/jneurosci.2045-11.2012>.
- Suzuki, N., Numakawa, T., Chou, J., de Vega, S., Mizuniwa, C., & Sekimoto, K., (2014). Teneurin-4 promotes cellular protrusion formation and neurite outgrowth through focal adhesion kinase signaling. *The FASEB Journal*, 28, 1386–1397. <https://doi.org/10.1096/fj.13-241034>.
- Tiklová, K., Björklund, Å.K., Lahti, L., Fiorenzano, A., Nolbrant, S., Gillberg, L., ... Perlmann, T. (2019). Single-cell RNA sequencing reveals midbrain dopamine neuron diversity emerging during mouse brain development. *Nature Communications*, 10, 581. <https://doi.org/10.1038/s41467-019-08453-1>.
- Van den Bos, R., Koot, S., & de Visser, L. (2014). A rodent version of the Iowa gambling task: 7 years of progress. *Frontiers in Psychology*, 5, 203. <https://doi.org/10.3389/fpsyg.2014.00203>.
- Varet, H., Brillet-Guéguen, L., Coppée, J. Y., & Dillies, M. A. (2016). SARTools: A DESeq2 and EdgeR-based R pipeline for comprehensive differential analysis of RNA-seq data. *Plos One*, 11, e0157022. <https://doi.org/10.1371/journal.pone.0157022>.
- Walker, D. M., Cates, H. M., Loh, Y. H. E., Purushothaman, I., Ramakrishnan, A., Cahill, K. M., ... Nestler, E. J. (2018). Cocaine self-administration alters transcriptome-wide responses in the brain's reward circuitry. *Biological Psychiatry*, 84, 867–880. <https://doi.org/10.1016/j.biopsych.2018.04.009>.
- Xue, C.-B., Xu, Z.-H., Zhu, J., Wu, Y., Zhuang, X.-H., Chen, Q.-L., ... Chen, J.-H. (2019). Exosome sequencing identifies TENM4 as a novel candidate gene for schizophrenia in the SCZD2 locus at 11q14-21. *Frontiers in Genetics*, 9, 725. <https://doi.org/10.3389/fgene.2018.00725>.
- Yokoyama, K., Kurihara, T., Saegusa, H., Zong, S., Makita, K., & Tanabe, T. (2004). Blocking the R-type CaV2.3 Ca²⁺ channel enhanced morphine analgesia and reduced morphine tolerance. *European Journal of Neuroscience*, 20, 3516–3519. <https://doi.org/10.1111/j.1460-9568.2004.03810.x>.
- Zeeb, F. D., Robbins, T. W., & Winstanley, C. A. (2009). Serotonergic and dopaminergic modulation of gambling behavior as assessed using a novel rat gambling task. *Neuropsychopharmacology*, 34, 2329–2343. <https://doi.org/10.1038/npp.2009.62>.
- Zhang, J., Tan, L., Ren, Y., Liang, J., Lin, R., Feng, Q., ... Luo, M. (2016). Presynaptic excitation via GABA_B receptors in habenula cholinergic neurons regulates fear memory expression. *Cell*, 166, 716–728. <https://doi.org/10.1016/j.cell.2016.06.026>.
- Zhou, Y., Zhou, B., Pache, L., Chang, M., Khodabakhshi, A. H., Tanaseichuk, O., ... Chanda, S. K. (2019). Metascape provides a biologist-oriented resource for the analysis of systems-level datasets. *Nature Communications*, 10, 1523. <https://doi.org/10.1038/s41467-019-09234-6>.

